Supporting Information

Revisiting the electrocatalytic hydrogenation of furfural to furfuryl alcohol using biomass-derived electrolytes

Maria Wolfsgruber, Robert H. Bischof, Christian Paulik, Adam Slabon and Bruno V. M. Rodrigues

Corresponding Authors

Bruno V. M. Rodrigues – Chair of Inorganic Chemistry, University of Wuppertal, Gaußstraße 20, 42119 Wuppertal, Germany. ORCID: 0000-0002-0130-8029.
Email: manzolli@uni-wuppertal.de
Phone-nr.: +49 202 4393435
Adam Slabon - Chair of Inorganic Chemistry, University of Wuppertal, Gaußstraße 20, 42119 Wuppertal, Germany; Wuppertal Center for Smart Materials & Systems, University of Wuppertal, 42119 Wuppertal, Germany. ORCID: 0000-0002-4452-1831.
Email: slabon@uni-wuppertal.de
Phone-nr.: +49202 4392517

Authors

Maria Wolfsgruber – Kompetenzzentrum Holz GmbH, c/o Werkstraße 2, 4860 Lenzing, Austria.
Robert H. Bischof – Lenzing AG, Werkstraße 2, 4860 Lenzing, Austria.
Christian Paulik – Institute for Chemical Technology of Organic Materials, Johannes Kepler University, Altenberger Straße 69, 4040 Linz, Austria.

Number of Pages: 10

Number of Tables: 3

Number of Figures: 5

Table of Contents

I. Supplemental Table

Table S1: Summary of literature reports on the electrochemical reduction of furfural to furfuryl alcohol, including different types of working electrodes (Nano-porous copper (Cu); Platinum (Pt), lanthanum doped titanium oxide (La-doped TiO_2), zinc (Zn), nickel (Ni), lead (Pb), silver-palladium alloy nanoparticles ($Ag_{60}Pd_{40}$ alloy NP), copper on N-doped hierarchically porous carbon (15%-Cu/NP_{900}), bimetallic copper- nickel catalyst on nickel foam (Cu-NPNi/NF), gold coated silver (Au-coated Ag)), counter electrodes and reference electrodes, the cell type and the solvents and electrolytes are listed. Furthermore the reaction temperature (T), the reaction time (RT), the yield of furfuryl alcohol(Y), the Faraday efficiency (FE) and the selectivity of furfuryl alcohol (S) are presented.

Lit. Nr.	WE	RE	CE	Process and cell-type	Solvent & Electrolyte	T/°C	RT	Y/%	FE/%	S/%
1[1]	Nano-porous copper (Cu)	Ag/AgCl	Pt	H-cell, fixed electrocat. process	Phosphate buffer solution (PBS), Methanol	25	2 h	35	51	51
2[1]	Nano-porous Cu	Ag/AgCl	Pt	H-cell, fluidized electrocat. process	PBS, Methanol	25	2 h	70	98	96
3[2]	Platinum (Pt)	Saturated calomel electrode (SCE)	Pt	H-cell	Sulphuric acid (H_2SO_4)	30	-	5	3	99
4[2]	3% Pt on activated carbon fiber	SCE	Pt	H-cell	Hydrochloric acid (HCl)	50	-	85	85	-
5[3]	La-doped TiO_2	SCE	Pt	H-cell	Dimethylformamide (DMF), tetra-butyl-ammonium bromide	25	-	89	86	-
6[4]	Cu	Graphite	-	Undivided cell	C_2H_5OK, Ethanol	Room temperature (RT)	5 h	31	60	-
7[4]	Cu	Graphite	-	Microchannel flow reactor	C_2H_5OK, Ethanol	RT	0.075mL/min for 10 min	90	90	-
8[5]	Zinc (Zn)	Graphite	Reversed hydrogen electrode (RHE)	H-cell	Sodium hydrogen carbonate ($NaHCO_3$)	RT	2 h	40	73	45
9[2]	Nickel (Ni)	SCE	Pt	H-cell	Sodium hydroxide (NaOH)	RT	-	20	16	25
10[6]	Lead (Pb)	SCE	Platinum-iridium sheet (Pt/Ir)	H-cell	H_2SO_4	RT	4 h	67	75	96
11[7]	$Ag_{60}Pd_{40}$ alloy NP	Ag/AgCl	Pt	H-cell	PBS	RT	1 h	0.2	95	3
12[8]	15%-Cu/NP_{900}	Ag/AgCl	Pt	H-cell	Potassium hydroxide (KOH)	RT	4 h	99	95	99
13[9]	Cu-NPNi/NF	Ag/AgCl	Pt	H-cell	NaOH	RT	1 h	54	54	74
Our work	Au-coated Ag	Ag/AgCl	Pt	H-cell	Sodium acetate (NaAc)	RT	2 h	35	79	54

Experiments 1-7 from the literature are discussed in detail in the manuscript. In experiments 8-10 and 13, the Faraday efficiencies (FEs) were lower than the FE obtained in our work (79%).[2,5,6,9] In experiment 8, zinc was used as the working electrode in an H-cell with sodium hydrogen carbonate as the electrolyte. The FE was 73%, and the selectivity was 45%.[5] Both values are lower compared to our study, where an FE of 79% and a selectivity

of 54% were achieved. The FE, yield, and selectivity in experiment 9 were all below 30%. The combination of nickel as the working electrode and sodium hydroxide as the electrolyte in an H-cell was worse for all three values than in our work.[2] Lead was used as the working electrode in experiment 10, with sulfuric acid as the electrolyte. Firstly, lead is toxic and therefore not suitable in biorefineries, and secondly, the FE in this experiment (75%) was below the FE in our work.[6] In experiment 11, the FE was higher than in our study, reaching 95%; however, the furfuryl alcohol yield was below 1% with the silver-palladium alloy electrocatalyst and a phosphate buffer as the electrolyte.[7] In experiment 12, a high FE of 95% and a high furfuryl alcohol yield of 99% were reported. However, when the experiment was repeated several times, inactivation of the copper on the N-doped hierarchically porous carbon electrocatalyst was observed after 8 cycles. The regeneration and production of the electrocatalyst are very complex. The 15% Cu/NC900 was produced by mixing NC900, melamine, $Cu(NO_3) \cdot 3\ H_2O$, and water for 2 hours. The mixture was heated to 85°C, and the temperature was held for 5 hours. The water was evaporated, and the solid residue was pyrolyzed at 600°C for 2 hours.[8] The bimetallic copper-nickel catalyst on nickel foam in literature experiment 13 had an FE of 54% with the sodium hydroxide electrolyte, and therefore, it was again below our FE.[9] In summary, our experiment presented the best combination of FE, furfuryl alcohol yield, and selectivity, in conjunction with sodium acetate as a green electrolyte and a gold-coated silver wire with good stability as the working electrode.

Table S2: Summary of the experiments (E1-E45) with different types of working electrodes (WE; Ag: silver, Sn: tin, CP: carbon paper, AucAg: gold-coated silver, Au: gold), the geometric surface areas of the WEs (A(WE)), the Potential (E), the different catholyte solutions and the stirrer speeds (v). All experiments were performed in an H-cell with a reaction time of 2 h. A three-electrode setup with a platinum mesh as the counter electrode and an Ag/AgCl (saturated KCl) the reference electrode was used.

Nr.	WE	A(WE)/cm^2	E/V *vs*. RHE	Catholyte solution	v/rpm
1	Ag	1	−0.6	LA+FF	200
2	Sn	1	−0.9	LA+FF	200
3	CP	1	−0.9	LA+FF	200
4	Ag	1	−0.6	HAc+FF	200
5	Sn	1	−0.9	HAc+FF	200
6	CP	1	−1.0	HAc+FF	200
7	AucAg	1	−0.6	HAc+FF	200
8	Au	1	−0.6	HAc+FF	200
9	Ag	1	−0.7	NaAc+FF	200
10	Sn	1	−0.7	NaAc+FF	200
11	AucAg	1	−0.7	NaAc+FF	200
12	CP	1	−1.0	NaAc+FF	200
13	CP	1	−0.7	NaAc+FF	200
14	Ag	1	−0.5	NaAc+FF	200
15	Au	1	−1.0	NaAc+FF	200
16	Sn	1	−1.1	NaAc+FF	200
17	AucAg	1	−0.5	1NaAc+FF	200
18	AucAg	1	−0.6	1NaAc+FF	200
19	AucAg	1	−0.7	1NaAc+FF	200
20	AucAg	1	−0.8	1NaAc+FF	200
21	AucAg	1	−0.9	1NaAc+FF	200
22	AucAg	1	−1.0	1NaAc+FF	200
23	AucAg	1	−1.1	1NaAc+FF	200
24	AucAg	1	−1.2	1NaAc+FF	200
25	AucAg	1	−1.3	1NaAc+FF	200
26	AucAg	1	−0.7	2NaAc+FF	200
27	AucAg	1	−0.7	3NaAc+FF	200
28	AucAg	1	−0.7	4NaAc+FF	200
29	AucAg	1	−0.7	4NaAc+FF	0
30	AucAg	1	−0.7	4NaAc+FF	100
31	AucAg	1	−0.7	4NaAc+FF	400
32	AucAg	1	−0.7	4NaAc+FF	600
33	AucAg	1	−0.7	4NaAc+FF	800
34	AucAg	1	−0.7	4NaAc+FF	1000
35	AucAg	1	−0.7	1NaAc+FF	100

36	AucAg	1	−0.7	1KAc+FF	100
37	AucAg	1	−0.7	4KAc+FF	100
38	AucAg	1	−0.8	1CsAc+FF	100
39	AucAg	1	−0.8	4CsAc+FF	100
40	AucAg	8	−0.7	1NaAc+FF	100
41	AucAg	8	−0.7	4NaAc+FF	100
42	AucAg	4	−0.7	1NaAc+FF	100
43	AucAg	4	−0.7	4NaAc+FF	100
44	AucAg	8	−0.7	1NaAc+FF	100
45	AucAg	8	−0.7	1NaAc+FF	100

Table S3: Results of the experiments (E1-E45) in the H-cell over a reaction time of 2 h. Platinum was used as the counter electrode and Ag/AgCl (saturated KCl) served as the reference electrode. Various working electrodes (WE; Ag: silver, Sn: tin, CP: carbon paper, AucAg: gold-coated silver, Au: gold) with different geometric surface areas of the WEs (A(WE)) and at multiple potentials (E) were tested. The influence of different catholyte solutions and stirrer speeds (v) was determined. The initial (c(FF)$_{init.}$) and the final (c(FF)$_{end}$) furfural concentrations, as well as the final furfuryl alcohol concentrations (c(FA)), were analysed. The total quantities of consumed electricity (Q), the furfuryl alcohol yields (Y(FA)), and the Faraday efficiencies (FEs) were determined.

Nr.	WE	A(WE)/cm²	E/V vs. RHE	Catholyte solution	v/rpm	c(FF)$_{init.}$/ mmol·L^{-1}	c(FF)$_{end}$/ mmol·L^{-1}	c(FA)/ mmol·L^{-1}	Y(FA)/%	FE/%	Q/A·s
1	Ag	1	−0.6	LA+FF	200	91	84	0.07	0.07	15	5
2	Sn	1	−0.9	LA+FF	200	92	82	-	-	-	-
3	CP	1	−0.9	LA+FF	200	90	80	-	-	-	-
4	Ag	1	−0.6	HAc+FF	200	94	86	0.07	0.07	15	4
5	Sn	1	−0.9	HAc+FF	200	94	86	-	-	-	-
6	CP	1	−1.0	HAc+FF	200	94	86	-	-	-	-
7	AucAg	1	−0.6	HAc+FF	200	92	86	0.09	0.10	17	5
8	Au	1	−0.6	HAc+FF	200	94	84	0.16	0.17	26	6
9	Ag	1	−0.7	NaAc+FF	200	92	71	0.21	0.22	7	30
10	Sn	1	−0.7	NaAc+FF	200	92	79	-	-	-	-
11	AucAg	1	−0.7	NaAc+FF	200	92	74	0.94	1.00	20	45
12	CP	1	−1.0	NaAc+FF	200	93	78	-	-	-	-
13	CP	1	−0.7	NaAc+FF	200	94	83	-	-	-	-
14	Ag	1	−0.5	NaAc+FF	200	94	85	0.05	0.06	13	4
15	Au	1	−1.0	NaAc+FF	200	93	64	0.34	0.36	4	87
16	Sn	1	−1.1	NaAc+FF	200	92	67	0.03	0.03	1	74
17	AucAg	1	−0.5	1NaAc+FF	200	94	88	0.18	0.18	27	6
18	AucAg	1	−0.6	1NaAc+FF	200	97	78	1.02	1.03	27	37
19	AucAg	1	−0.7	1NaAc+FF	200	110	76	6.76	6.03	58	112
20	AucAg	1	−0.8	1NaAc+FF	200	101	66	5.74	5.58	42	132
21	AucAg	1	−0.9	1NaAc+FF	200	110	61	5.81	5.19	34	167
22	AucAg	1	−1.0	1NaAc+FF	200	99	55	7.96	7.91	38	205
23	AucAg	1	−1.1	1NaAc+FF	200	111	58	8.83	7.80	38	224
24	AucAg	1	−1.2	1NaAc+FF	200	94	47	7.68	7.96	22	335
25	AucAg	1	−1.3	1NaAc+FF	200	99	48	7.67	7.62	16	476
26	AucAg	1	−0.7	2NaAc+FF	200	102	83	4.14	3.98	70	57
27	AucAg	1	−0.7	3NaAc+FF	200	100	84	2.66	2.60	67	39
28	AucAg	1	−0.7	4NaAc+FF	200	96	78	3.63	3.69	75	47
29	AucAg	1	−0.7	4NaAc+FF	0	97	83	2.11	2.13	77	26
30	AucAg	1	−0.7	4NaAc+FF	100	97	83	2.82	2.85	81	34
31	AucAg	1	−0.7	4NaAc+FF	400	103	76	4.07	3.85	74	53
32	AucAg	1	−0.7	4NaAc+FF	600	94	72	3.51	3.67	73	47
33	AucAg	1	−0.7	4NaAc+FF	800	99	75	2.59	2.57	63	50
34	AucAg	1	−0.7	4NaAc+FF	1000	94	70	2.89	3.02	62	45
35	AucAg	1	−0.7	1NaAc+FF	100	99	73	8.47	8.36	73	112
36	AucAg	1	−0.7	1KAc+FF	100	99	71	7.89	7.84	65	118
37	AucAg	1	−0.7	4KAc+FF	100	94	72	4.47	4.67	78	55
38	AucAg	1	−0.8	1CsAc+FF	100	97	72	6.80	6.86	56	118

39	AucAg	1	−0.8	4CsAc+FF	100	94	75	3.86	4.04	54	69
40	AucAg	8	−0.7	1NaAc+FF	100	99	38	37.50	37.20	82	444
41	AucAg	8	−0.7	4NaAc+FF	100	98	61	19.29	19.29	88	213
42	AucAg	4	−0.7	1NaAc+FF	100	98	54	18.36	18.34	71	251
43	AucAg	4	−0.7	4NaAc+FF	100	97	64	11.97	12.06	74	155
44	AucAg	8	−0.7	1NaAc+FF	100	98	30	37.09	37.00	86	415
45	AucAg	8	−0.7	1NaAc+FF	100	100	36	32.65	31.80	70	453

II.   Supplemental Figures
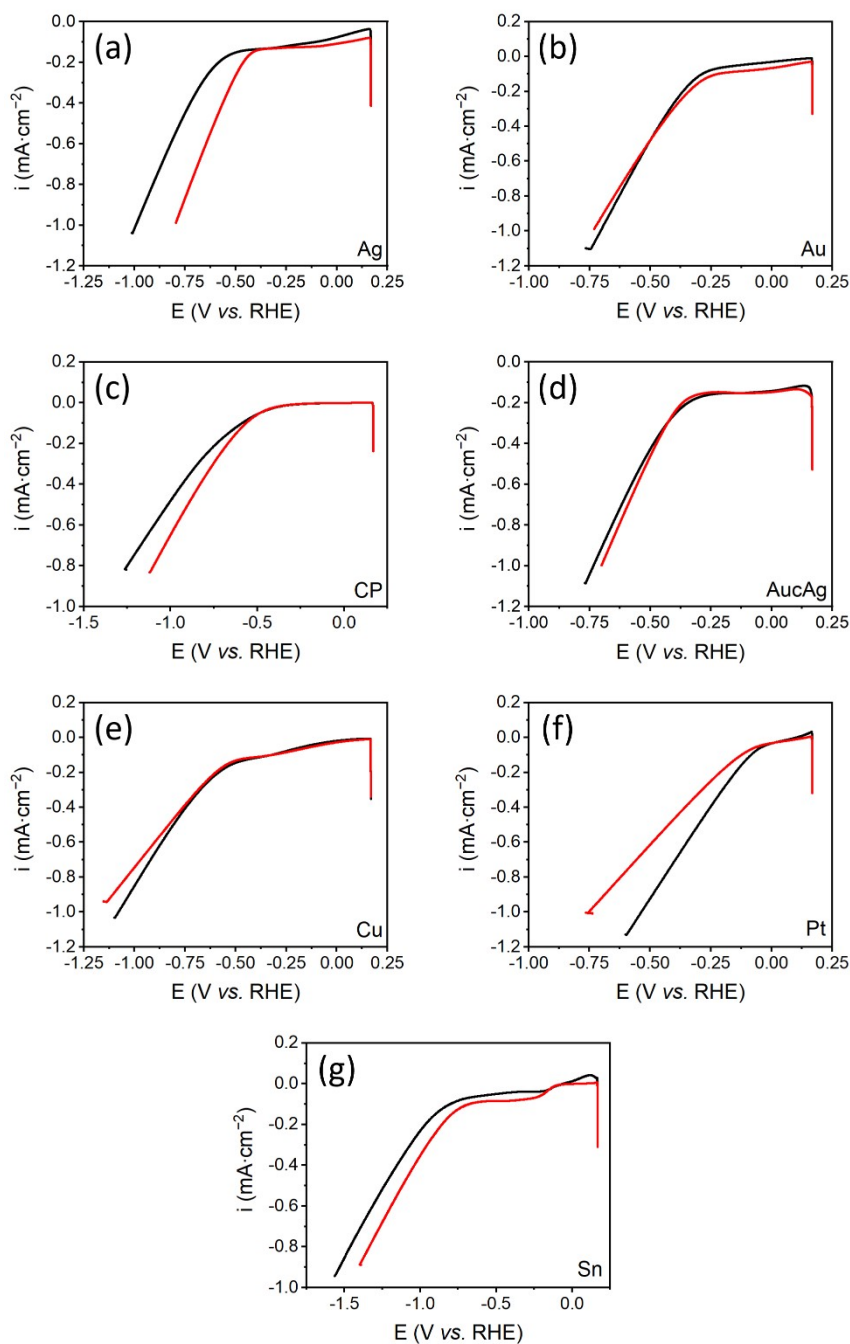
Figure S1. Linear sweep voltammetry curves with 0.1 M acetic acid (black line) and 0.1 M furfural with 0.1 M acetic acid (red line) are depicted. The reaction was performed in an H-cell with Ag/AgCl (saturated KCl) as the reference electrode and Pt as the counter electrode. The working electrodes had a geometric surface area of 1 cm^2, and (a) Ag, (b) Au, (c) CP, (d) AucAg, (e) Cu, (f) Pt, and (g) Sn were tested.
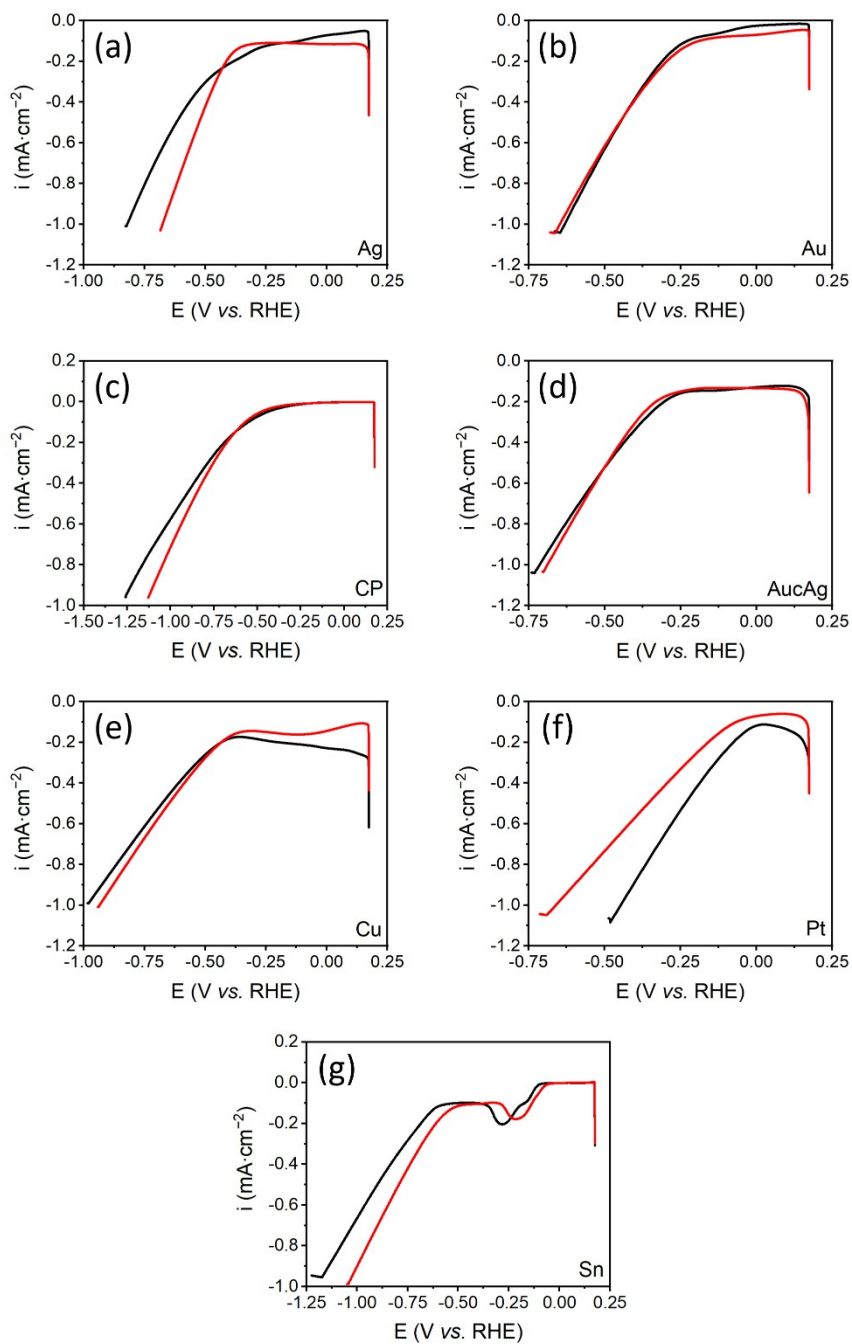
Figure S2. Linear sweep voltammetry curves with 0.1 M levulinic acid (black line) and 0.1 M furfural with 0.1 M levulinic acid (red line) are shown. Ag/AgCl (saturated KCl) was used as the reference electrode and Pt as the counter electrode, respectively. The experiments were performed in an H-cell. The working electrodes were (a) Ag, (b) Au, (c) CP, (d) AucAg, (e) Cu, (f) Pt, and (g) Sn; all with a geometric surface area of 1 cm^2.
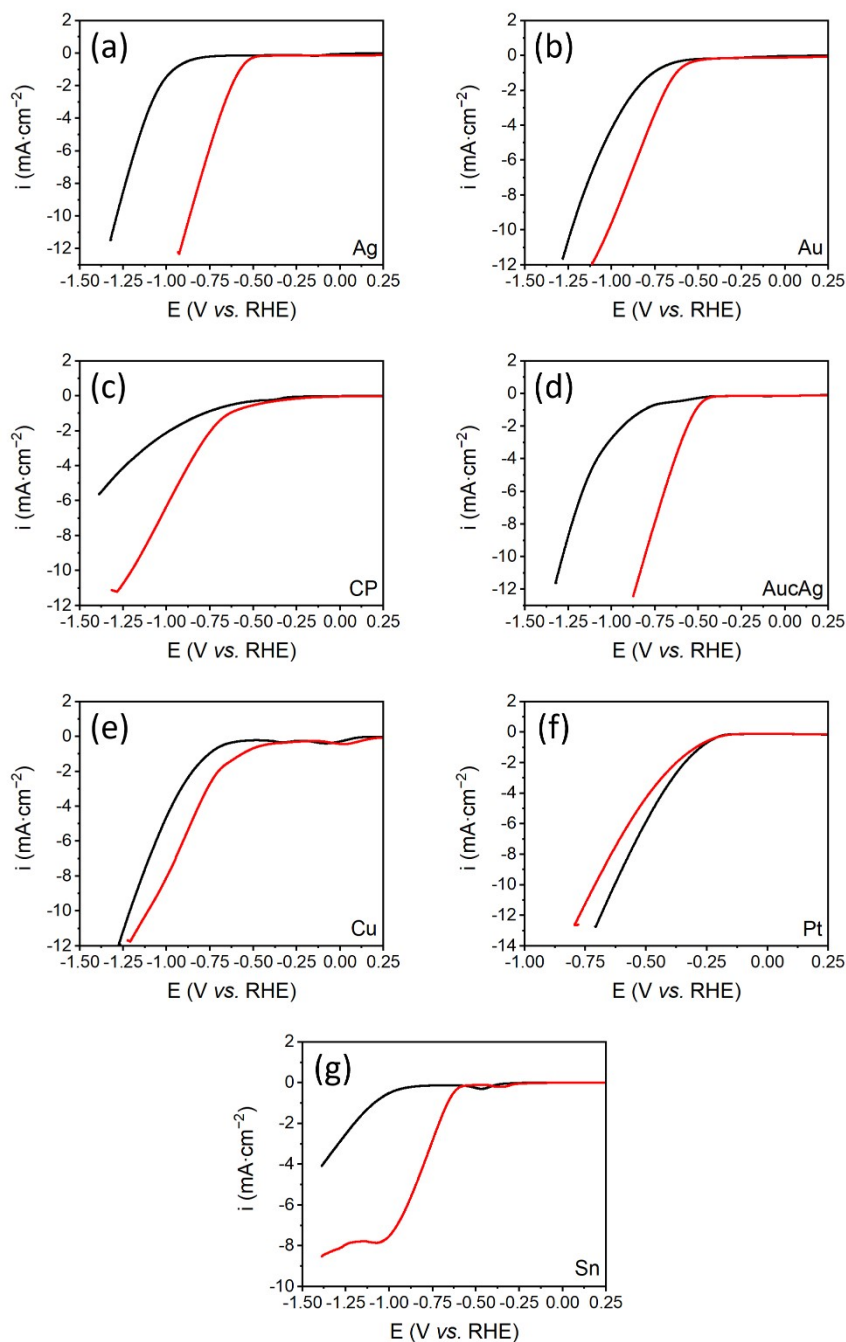
Figure S3. Linear sweep voltammetry curves with 0.1 M sodium acetate (black line) and 0.1 M furfural with 0.1 M sodium acetate (red line) in an H-cell are presented. A three-electrode setup with Ag/AgCl (saturated KCl) as the reference electrode and Pt as the counter electrode was used. The working electrodes were (a) Ag, (b) Au, (c) CP, (d) AucAg, (e) Cu, (f) Pt, and (g) Sn. The working electrodes had geometric surface areas of 1 cm^2.

In the linear sweep voltammograms conducted with acetic acid as the electrolyte, both the potentials and current densities remained relatively stable for Au and AucAg electrocatalysts, regardless of the presence of furfural. However, Ag, CP, and Sn electrocatalysts exhibited a shift towards more positive potentials and higher current densities in the presence of furfural. Conversely, Cu and Pt electrocatalysts showed a more negative onset potential and lower current densities when furfural was introduced. Similar trends were observed when levulinic acid was used as the electrolyte, with the behavior of the electrocatalysts mirroring that observed with acetic acid. Notably, Cu demonstrated a distinct shift towards more positive potentials and higher current densities in the presence of furfural. When sodium acetate was employed as the electrolyte, a general trend emerged where the potentials shifted towards more positive values, and current densities increased for Ag, Au, AucAg, Cu, CP, and Sn electrocatalysts in the presence of furfural. Conversely, Pt displayed a more negative potential and lower current densities under the same conditions. Liu *et al.* previously investigated the behavior of various electrocatalysts in the reduction of furfural to furfuryl alcohol, providing a basis for comparison with the observed linear sweep voltammograms.[10] The following descriptions pertain to the various curve shapes observed with and without furfural across all electrocatalysts and electrolytes. These variations in curve shapes may be

attributed to differences in reaction mechanisms and intermediates formed during the reaction process. A shift towards more positive potentials and an increase in current densities in the presence of furfural typically indicate that the initial step of the reduction reaction involves the formation of a carbon radical on the aldehyde group, with protons obtained directly from water. Subsequently, furfuryl alcohol is synthesized with a proton adsorbed on the electrocatalyst surface. Conversely, when potentials and current densities remain largely unchanged with furfural, it suggests that a proton adsorbed directly on the electrocatalyst facilitates the formation of the carbonyl radical on the aldehyde group. This is followed by a second adsorbed proton reacting with the radical to produce furfuryl alcohol. The presence of organic adsorbates can inhibit electrode activity, resulting in a shift of the onset potential towards more negative values and lower current densities in the presence of furfural. This hindrance in the reduction of furfural to furfuryl alcohol prevents the reaction from proceeding effectively on certain electrocatalysts, leading to more negative potentials and lower current densities. Overall, these observations shed light on the intricate mechanisms governing the reduction of furfural to furfuryl alcohol on various electrocatalytic surfaces.[10]
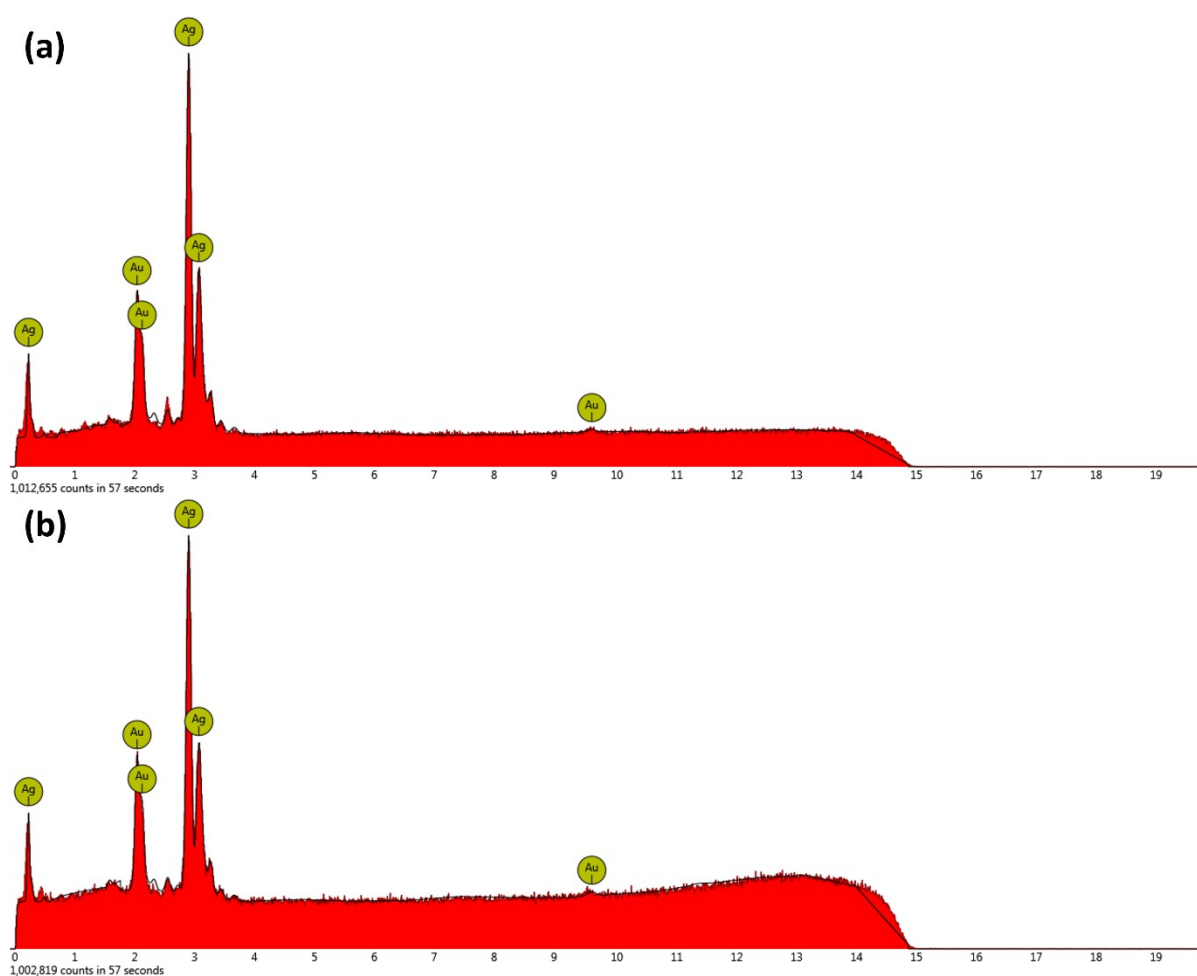

Figure S4. EDS spectra of the AucAg WE (a) before and (b) after the reaction with 0.1 M furfural to furfuryl alcohol. The WE with a geometric surface area of 8 cm² was used for the reaction performed in an H-cell at −0.7 V *vs*. RHE (pH 8.7). The electrolyte concentration was 1.0 M NaAc and the reaction time was 2 h. A setup of Ag/AgCl (saturated KCl) was used as RE and platinum as CE, respectively.
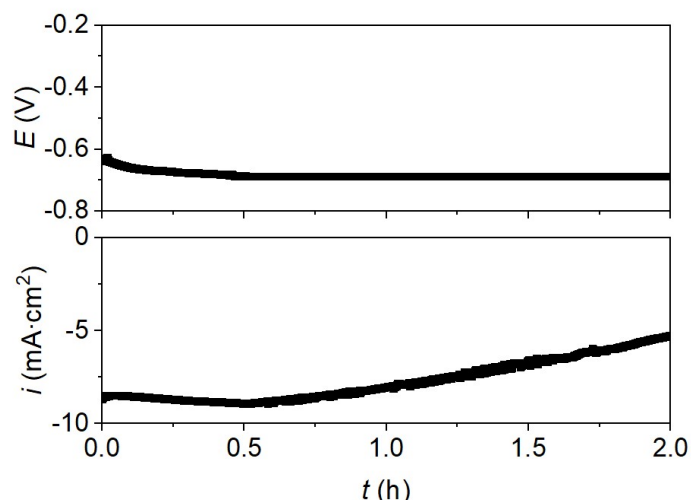
Figure S5. Chronoamperometric spectra of the best experiment with the reaction of 0.1 M furfural to furfuryl alcohol. A setup of AucAg was used as WE (geometric surface area of 8 cm²), Ag/AgCl (saturated KCl) as RE and platinum as CE, respectively. The reaction was performed in an H-cell at −0.7 V *vs*. RHE (pH 8.7). The electrolyte concentration was 1.0 M NaAc and the reaction time was 2 h. The upper part shows the applied potential *versus* the time and the lower part the measured current density *versus* the time.

III.   Faraday efficiency and furfuryl alcohol yield

The Faraday efficiency (FE) was calculated using Equation S1:

$$FE = \frac{n(FA) \cdot z \cdot F}{I \cdot t} \cdot 100\% = \frac{c(FA) \cdot V \cdot z \cdot F}{Q} \cdot 100\%$$
Eq. S1

where $n(FA)$ is the produced amount of furfuryl alcohol (mol), z is the number of electrons for the conversion of one molecule of furfural to one molecule of furfuryl alcohol ($z = 2$), F is the Faraday constant (96485 C·mol⁻¹), I is the current (A), t the reaction time (s), $c(FA)$ is the produced furfuryl alcohol concentration (mol·L⁻¹), V is the volume of the solution in the catholyte chamber (L), and Q is the quantity of consumed electricity (C).

The furfuryl alcohol yield $Y(FA)$ was determined based on Equation S2:

$$Y(FA) = \frac{c(FA) \cdot V}{c(FF) \cdot \frac{M(FA)}{M(FF)} \cdot V} \cdot 100\%$$
Eq. S2

where $c(FA)$ is the produced furfuryl alcohol concentration (mol·L⁻¹), V is the volume of the catholyte solution (L), $c(FF)$ is the initial furfural concentration (mol·L⁻¹), $M(FA)$ is the molar mass of furfuryl alcohol (g·mol⁻¹), and $M(FF)$ is the molar mass of furfural (g·mol⁻¹).

References

(1) Yang, Z.; Chou, X.; Kan, H.; Xiao, Z.; Ding, Y. Nanoporous Copper Catalysts for the Fluidized Electrocatalytic Hydrogenation of Furfural to Furfuryl Alcohol. *ACS Sustain. Chem. Eng.* **2022**, *10* (22), 7418–7425. DOI: 10.1021/acssuschemeng.2c02360.

(2) Zhao, B.; Chen, M.; Guo, Q.; Fu, Y. Electrocatalytic hydrogenation of furfural to furfuryl alcohol using platinum supported on activated carbon fibers. *Electrochim. Acta* **2014**, *135*, 139–146. DOI: 10.1016/j.electacta.2014.04.164.

(3) Wang, F.; Xu, M.; Wei, L.; Wei, Y.; Hu, Y.; Fang, W.; Zhu, C. G. Fabrication of La-doped TiO2 Film Electrode and investigation of its electrocatalytic activity for furfural reduction. *Electrochim. Acta* **2015**, *153*, 170–174. DOI: 10.1016/j.electacta.2014.11.203.

(4) Cao, Y.; Noël, T. Efficient Electrocatalytic Reduction of Furfural to Furfuryl Alcohol in a Microchannel Flow Reactor. *Org Process Res Dev* **2019**, *23* (3), 403–408. DOI: 10.1021/acs.oprd.8b00428. Published Online: Feb. 8, 2019.

(5) Dhawan, M. S.; Yadav, G. D.; Calabrese Barton, S. Zinc-electrocatalyzed hydrogenation of furfural in near-neutral electrolytes. *Sustain. Energy Fuels* **2021**, *5* (11), 2972–2984. DOI: 10.1039/D1SE00221J.

(6) Parpot, P.; Bettencourt, A.; Chamoulaud, G.; Kokoh, K.; Belgsir, E. Electrochemical investigations of the oxidation–reduction of furfural in aqueous medium: Application to electrosynthesis. *Electrochim. Acta* **2004**, *49* (3), 397–403. DOI: 10.1016/j.electacta.2003.08.021.

(7) Brosnahan, J. T.; Zhang, Z.; Yin, Z.; Zhang, S. Electrocatalytic reduction of furfural with high selectivity to furfuryl alcohol using AgPd alloy nanoparticles. *Nanoscale* **2021**, *13* (4), 2312–2316. DOI: 10.1039/d0nr07676g.

(8) Xu, W.; Yu, C.; Chen, J.; Liu, Z. Electrochemical hydrogenation of biomass-based furfural in aqueous media by Cu catalyst supported on N-doped hierarchically porous carbon. *Applied Catalysis B: Environmental* **2022**, *305*, 121062. DOI: 10.1016/j.apcatb.2022.121062.

(9) Dixit, R. J.; Bhattacharyya, K.; Ramani, V. K.; Basu, S. Electrocatalytic hydrogenation of furfural using non-noble-metal electrocatalysts in alkaline medium. *Green Chem.* **2021**, *23* (11), 4201–4212. DOI: 10.1039/D1GC00579K.

(10) Liu, L.; Liu, H.; Huang, W.; He, Y.; Zhang, W.; Wang, C.; Lin, H. Mechanism and kinetics of the electrocatalytic hydrogenation of furfural to furfuryl alcohol. *J. Electroanal. Chem.* **2017**, *804*, 248–253. DOI: 10.1016/j.jelechem.2017.09.021.